

# STRUCTURE OF Bi<sub>2</sub>O<sub>3</sub>–SiO<sub>2</sub> GLASSES

Tokuro Nanba\*, Hiroyasu Tabuchi and Yoshinari Miura

*Department of Environmental Chemistry and Materials, Okayama University,*

*Okayama 700-8530, Japan*

tokuro\_n@cc.okayama-u.ac.jp

While Bi<sub>2</sub>O<sub>3</sub> has been so far regarded as a conditional glass former, the structural role of Bi ions in the bismuthate glasses has been still obscure. In the present study, Bi<sub>2</sub>O<sub>3</sub>–SiO<sub>2</sub> system was chosen to investigate the glass structure. According to <sup>29</sup>Si MAS-NMR and X-ray radial distribution analyses, similarities in local structure around bismuth and oxygen sites were confirmed between 50Bi<sub>2</sub>O<sub>3</sub>·50SiO<sub>2</sub> glass and a Bi<sub>2</sub>SiO<sub>5</sub> crystal. It was concluded that Bi–O–Bi networks were commonly present in Bi<sub>2</sub>O<sub>2</sub> layers and 1-dimensional SiO<sub>3</sub> chains interlinked the layers. It was also concluded that Si–O–Si networks were indispensable for the glass formation

(Keywords: glass structure, NMR, XPS, diffraction method)

## 1. Introduction

Pb-containing glasses have excellent properties, such as high refractive indices and low melting temperatures, and hence they have been widely used in various applications, such as table wares, optical lenses and solder glasses for electronic components. Bi and Pb are placed next to each other on the periodic table, and Bi<sup>3+</sup> and Pb<sup>2+</sup> ions have the same 6s<sup>2</sup> electronic configurations. Therefore, a number of similarities have been confirmed in various properties. In toxicity, however, Bi is much safer than Pb. For these reasons, Bi-based materials have been expected as substitutes for the Pb-containing materials, and the novel glass systems have been explored in glass industries.

It is well known that Bi<sub>2</sub>O<sub>3</sub> does not vitrify without additives, but the addition of other oxides enables its vitrification. It has been reported that Bi ions in oxide glasses have 5- or 6-fold coordination state [1]. Bi ions in trivalent state possess lone pair electrons in the outer most 6s<sup>2</sup> shell. It has been accepted that the 6s<sup>2</sup> lone pair electrons are localized on Bi ions and they do not partake in Bi–O bonds. It has been also accepted that BiO<sub>*n*</sub> polyhedra were distorted due to the lone pair electrons, and the distortion in BiO<sub>*n*</sub> units would make the structural analyses for the Bi-containing glasses difficult.

According to radial distribution analyses, Watanabe et al. [2] revealed that Bi<sub>2</sub>O<sub>3</sub>–Li<sub>2</sub>O glass had a similar structure to a Bi<sub>2</sub>O<sub>4</sub> crystal. In Bi<sub>2</sub>O<sub>4</sub> crystal, Bi ions are in a mixed valence state of 3+ and 5+, and in the Bi<sub>2</sub>O<sub>3</sub>–Li<sub>2</sub>O glass, however, it was confirmed that Bi ions were all in a trivalent state and large amount of defects, such as positive electron holes on oxide ions were

present in the glass. It was expected that Bi ions played a role as a network former, NWF in the Bi<sub>2</sub>O<sub>3</sub>–Li<sub>2</sub>O glass. While coordination number of Bi ions has been reported in the combination of some typical NWFs such as B<sub>2</sub>O<sub>3</sub> and P<sub>2</sub>O<sub>5</sub> [3–5], structural roles of Bi ions have not been clarified. In the present study, Bi<sub>2</sub>O<sub>3</sub>–SiO<sub>2</sub> system was chosen to examine the glass structure, where the structural information was collected from the spectroscopic methods such as optical absorption, <sup>29</sup>Si MAS-NMR and XPS, and the radial distribution analyses were also performed from X-ray diffraction measurements. According to the information, the structural role of Bi ions in the glass formation was discussed.

## 2. Experimental

The glasses were prepared in the composition of *x*Bi<sub>2</sub>O<sub>3</sub>·(100–*x*)SiO<sub>2</sub> (*x* = 35 – 65 mol%), and 0.1 mol% Fe<sub>2</sub>O<sub>3</sub> was also added to the batches for reducing the spin lattice relaxation time in <sup>29</sup>Si MAS-NMR measurements. At *x* = 35, 40 and 50, the batches were melted at 1050 – 1200 °C in a Pt crucible, and at *x* = 60 and 65, they were melted at 950 – 1010 °C in a Au crucible. The melts were press-quenched by Cu plates, and sometimes the crucible bottom was dipped in water obtaining higher quenching rate.

The glasses obtained were evaluated by various methods. Thermo-gravimetric analysis (TGA) and differential thermal analysis (DTA) were performed under the atmospheres of dry air and nitrogen flow. Diffuse reflectance spectra of the powdered specimens were measured with a spectrophotometer equipped with an integrating sphere, and the reflectance spectra measured were converted into absorption spectra by using a

Kubelka-Munk function. XPS measurements were carried out, where the glass samples were fractured in an ultrahigh vacuum ( $\sim 1 \times 10^{-7}$  Pa), and the fresh surfaces were immediately analyzed to prevent surface degradation. A monochromatic Al-K $\alpha$  ( $h\nu = 1486.6$  eV) was irradiated to the fresh surfaces, and the surface charge was controlled by means of covering the surface with an electrically grounded Ni mesh screen as well as flooding with low energy electrons ( $\sim 5$  eV) [6]. Crystal powders were also analyzed applying the same charge neutralization method. C1s peak of an adventitious hydrocarbon was adopted as a calibration standard (284.6 eV).  $^{29}\text{Si}$  MAS-NMR spectra were obtained at 59.6 MHz (7.05 T) with 5.0  $\mu\text{s}$  pulses and 1.0 s recycle delays. The chemical shift standards used were poly (dimethyl siloxane) (PDMS). X-ray scattering measurement was carried out with powdered specimens, being irradiated with a monochromatic Mo-K $\alpha$  ( $\lambda = 0.7107$  Å) radiation. Total correlation function,  $T(r) = 4\pi r\rho(r)$ , and differential correlation function,  $D(r) = 4\pi r[\rho(r) - \rho_0]$ , were obtained by a Fourier transformation of the interference function, where  $\rho(r)$  is the density function,  $\rho_0$  is the average number

density and  $r$  is the distance from any reference atom center. Reliability of the data was checked by reverse Fourier transformation. XPS and  $^{29}\text{Si}$  MAS-NMR measurements were done for  $\text{PbO-SiO}_2$  glasses, making a comparison in local structures.

### 3. Results

Optical absorption spectra were measured in order to evaluate the valency of Bi ions. As shown in Fig. 1, the absorption edge of the present glasses are located at around 3 eV, which is almost the same with the bismuthate crystals,  $\text{Bi}_2\text{O}_3$  and  $\text{Bi}_4(\text{SiO}_4)_3$  containing  $\text{Bi}^{3+}$  ions. It is therefore concluded that Bi ions in the glasses are present in a trivalent state and the amount of  $\text{Bi}^{5+}$  ions are negligible if present. Furthermore, neither weight gains under air flow nor weight losses under  $\text{N}_2$  flow were confirmed in TG measurements, leading to a conclusion that positive electron holes on oxide ions and oxygen defects which have been confirmed in  $\text{Bi}_2\text{O}_3\text{-Li}_2\text{O}$  glass were negligible in the present  $\text{Bi}_2\text{O}_3\text{-SiO}_2$  glass.

Fig. 2 shows O1s XPS spectra. With increasing  $\text{Bi}_2\text{O}_3$  content, the O1s signal shifts to the lower binding energy side, indicating the increase in polarizability of oxide ions due to the addition of Bi ions with higher polarizability. In the present glasses, oxide ions are classified into three groups, Si-O-Si, Si-O-Bi and Bi-O-Bi. In the observed O1s XPS spectra, however, only two components are extracted. The lower binding

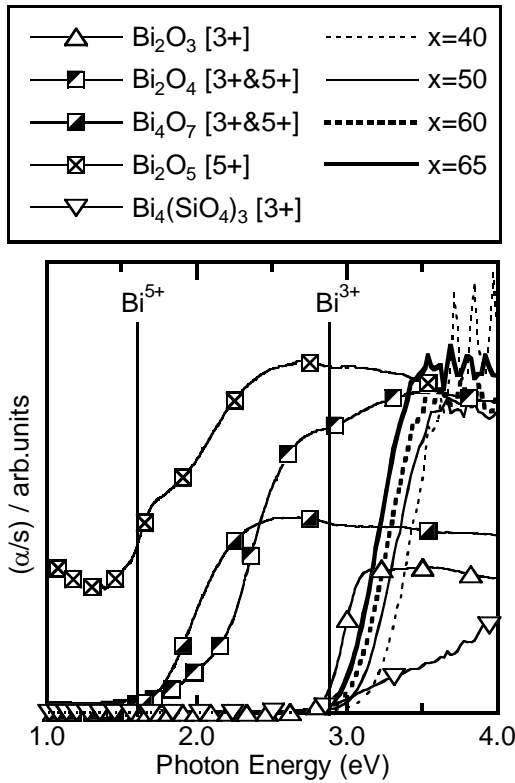


**Fig. 1.** Optical absorption spectra obtained from the diffuse reflectance measurements for  $x\text{Bi}_2\text{O}_3 \cdot (100-x)\text{SiO}_2$  glasses and the bismuthate crystals with various valence states of Bi ions.

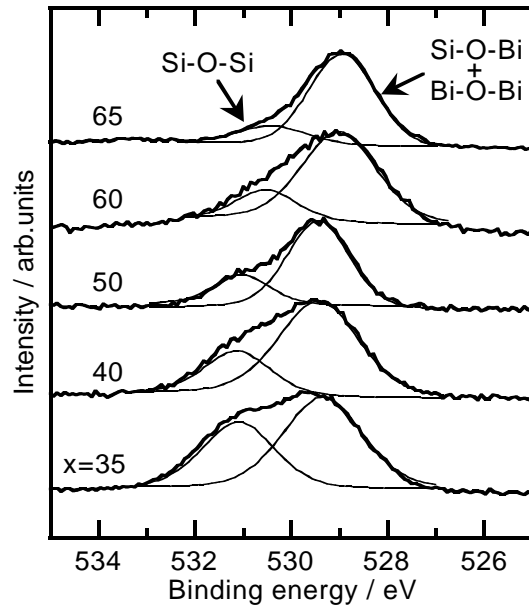


**Fig. 2.** O1s XPS spectra and the separated components for  $x\text{Bi}_2\text{O}_3 \cdot (100-x)\text{SiO}_2$  glasses.

energy component is attributed to the oxide ions in Si–O–Bi and Bi–O–Bi groups. It is expected that Bi–O bonds have much higher  $\pi$ -bonding character than Si–O bonds, because the vacant Bi6d orbitals spread out more widely than Si3d. It is therefore supposed that electrons on oxide ions are delocalized through the vacant Bi6d orbitals, and the oxide ions adjacent to Bi ions are equalized in electron density, being observed as one component in the O1s signal. It is therefore concluded that the higher binding energy component is attributable to the oxide ions in Si–O–Si units and the lower energy component is to those in Si–O–Bi and Bi–O–Bi units.

Fig. 3 shows  $^{29}\text{Si}$  MAS-NMR spectra. The relative amounts of  $Q_n$  species ( $\text{SiO}_4$  units containing  $n$  bridging oxygens) were obtained from the peak separation. As far as known to the authors,  $^{29}\text{Si}$  NMR studies on the  $\text{Bi}_2\text{O}_3$ – $\text{SiO}_2$  system have never been published. Therefore, among the  $\text{PbO}$ – $\text{SiO}_2$  systems [7–9], the  $^{29}\text{Si}$  chemical shifts in a  $\text{PbF}_2$ – $\text{PbO}$ – $\text{SiO}_2$  system [7] were chosen as the initial entries for the peak separations, which were shown as the vertical lines in Fig. 3. The results of the deconvolutions are summarized in Table 1. The relative amounts of bridging oxygens in Si–O–Si units are estimated from the deconvolutions results, and they are shown in Fig. 4 together with the data evaluated from XPS. The amounts of Si–O–Si

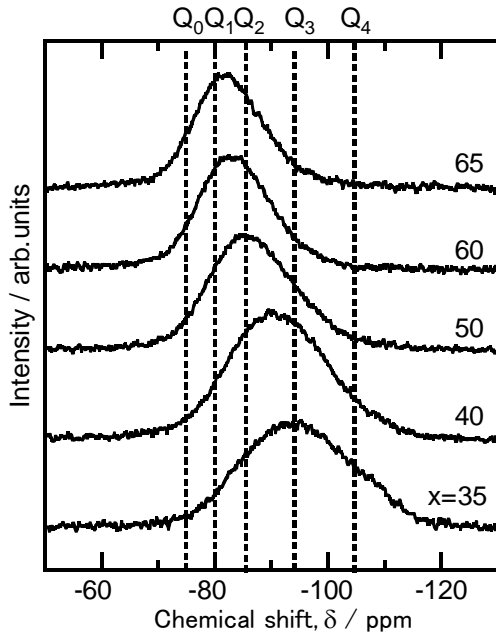


**Fig. 3.**  $^{29}\text{Si}$  MAS-NMR spectra at 7.05 T for  $x\text{Bi}_2\text{O}_3 \cdot (100-x)\text{SiO}_2$  glasses. The vertical lines indicate the  $^{29}\text{Si}$  chemical shifts of  $Q_n$  units in  $\text{PbF}_2$ – $\text{PbO}$ – $\text{SiO}_2$  glasses [7].

**Table 1.** Isotropic chemical shifts ( $\delta$  / ppm) and relative intensities ( $I$  / %) of  $Q_n$  units in  $x\text{Bi}_2\text{O}_3 \cdot (100-x)\text{SiO}_2$  glasses. The uncertainties are 0.5 ppm for  $\delta$  and 2% for  $I$ .

$x$	$Q_4$		$Q_3$		$Q_2$		$Q_1$		$Q_0$	
	$-\delta$	$I$								
35	105.1	26	95.9	37	87.7	31	78.8	6		
40	104.5	13	95.5	36	87.1	41	78.8	10		
50	104.0	5	93.2	28	85.6	43	79.3	24		
60			91.6	18	85.1	40	79.7	38	74.6	4
65			91.4	16	84.8	33	79.4	45	74.7	6

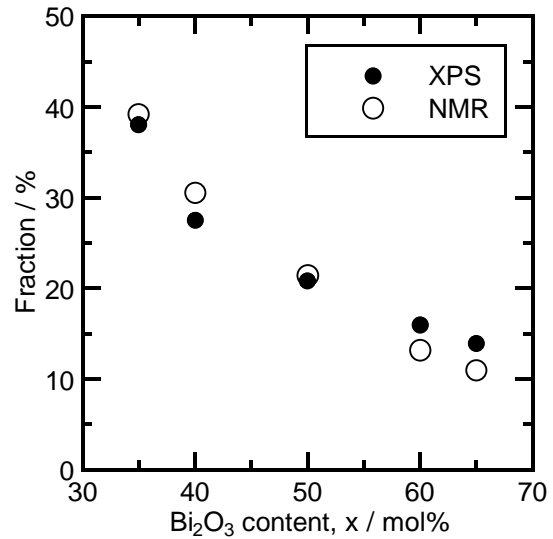


**Fig. 4.** Relative amount of oxide ions in Si–O–Si bridges determined from O1s XPS and  $^{29}\text{Si}$  NMR in  $x\text{Bi}_2\text{O}_3 \cdot (100-x)\text{SiO}_2$  glasses. The uncertainties are 2% in XPS and 5% in NMR.

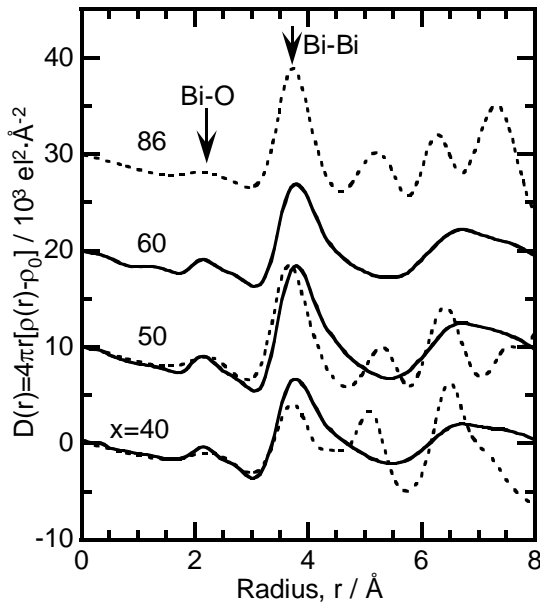
bridges are in good agreement between XPS and NMR, indicating that the deconvolutions and the subsequent assignments in XPS and NMR are appropriate for the present  $\text{Bi}_2\text{O}_3$ – $\text{SiO}_2$  glasses.

Fig. 5 shows the differential correlation functions,  $D(r)$ s obtained from X-ray diffraction measurements. The peaks seen at 2.3 and 3.8 Å are assigned to the neighboring Bi–O and Bi–Bi pairs. With increasing  $\text{Bi}_2\text{O}_3$  content, a broad shoulder at around 2.7 Å increases in intensity, suggesting the wider distribution of Bi–O bond length and the distortion of  $\text{BiO}_n$  polyhedra. The peaks of Si–O bonds are supposed to be observed at 1.6 Å but are not clearly seen in Fig. 5, which is due to the large difference in scattering coefficient between Bi and Si atoms. Then, the coordination numbers only around Bi ions are evaluated from the RDFs (Table 2). At  $x = 50$ , the coordination numbers,  $N_{\text{Bi}}(\text{O})$  and  $N_{\text{Bi}}(\text{Bi})$  are approximately consistent between the glass and

crystal, suggesting the similarity in coordination structure around Bi ions. In RDFs, however, a peak at around 5 Å is commonly observed for the crystals (dotted lines), while no peak is seen for the glasses (solid lines). In the crystals, the 5 Å peak is attributed to the second neighboring Bi–Bi pairs across SiO<sub>4</sub> or BiO<sub>n</sub> units,  $\underline{\text{Bi}}-(\text{Si}/\text{Bi})-\underline{\text{Bi}}$ . It is therefore expected that random distribution of the second neighboring BiO<sub>n</sub> units results in the broadening and weakening of the 5 Å peak for the glasses.

**Table 2.** Number of the nearest neighbors around Bi ions,  $N_{\text{Bi}}$  for  $x\text{Bi}_2\text{O}_3 \cdot (100-x)\text{SiO}_2$  glasses, which was estimated from a peak fitting (uncertainty =  $\pm 0.2$ ). The  $N_{\text{Bi}}$  values in the bismuth silicate crystals,  $\text{Bi}_4(\text{SiO}_4)_3$ ,  $\text{Bi}_2\text{SiO}_5$  and  $\text{Bi}_{12}\text{SiO}_{20}$  are also shown in the parentheses.

$x$	35	40	50	60	86
$N_{\text{Bi}}(\text{O})$	6.0	6.1 (6.0)	6.3 (6.0)	6.7	— (7.0)
$N_{\text{Bi}}(\text{Bi})$	7.4	7.6 (5.0)	8.0 (8.0)	9.4	— (10.0)



**Fig. 5.** Differential correlation functions,  $D(r)$  for  $x\text{Bi}_2\text{O}_3 \cdot (100-x)\text{SiO}_2$  glasses (solid lines, experiment) and the bismuth silicate crystals,  $\text{Bi}_4(\text{SiO}_4)_3$  ( $x=40$ ),  $\text{Bi}_2\text{SiO}_5$  ( $x=50$ ) and  $\text{Bi}_{12}\text{SiO}_{20}$  ( $x=86$ ) (dotted lines, simulation).

#### 4. Discussion

From the  $Q_n$  distributions determined from  $^{29}\text{Si}$  NMR analyses (Table 1), the amounts of oxide ions in the structural groups, Si–O–Si and Si–O–Bi are estimated, where it is assumed that oxide ions in the Si–O–Bi units were regarded as NBOs in  $^{29}\text{Si}$  NMR. The residuals are attributable to the oxide ions not bonding to Si atoms, that is, oxide ions in Bi–O–Bi

units. Fig. 6 shows the relative amount of oxide ions in Si–O–Si, Si–O–Bi and Bi–O–Bi units estimated in this way, and the results for PbO–SiO<sub>2</sub> glass are also shown in Fig. 6. As shown by the dotted line, all the bridging Si–O–Si oxygens would turn into non-bridging Si–O–(Bi,Pb) oxygens at O/Si ratio = 4.0, if Bi and Pb ions acted as a network modifier, NWM. In practice, however, 30% of oxide ions are present as bridging oxygen at O/Si = 4.0 ( $40\text{Bi}_2\text{O}_3 \cdot 60\text{SiO}_2$ ). The deviation from the theoretical line indicates the formation of oxygens not bonding to Si atoms, that is, the formation of Bi–O–Bi networks. In the high Bi<sub>2</sub>O<sub>3</sub> content glasses ( $x \geq 60$ ), over 50% of oxygens are present in the Bi–O–Bi networks. It is also noted that the Si–O–Si bridges remain even at the upper limit of the glass forming region (O/Si = 7.6), suggesting that the Si–O–Si bridges are indispensable to the glass formation.

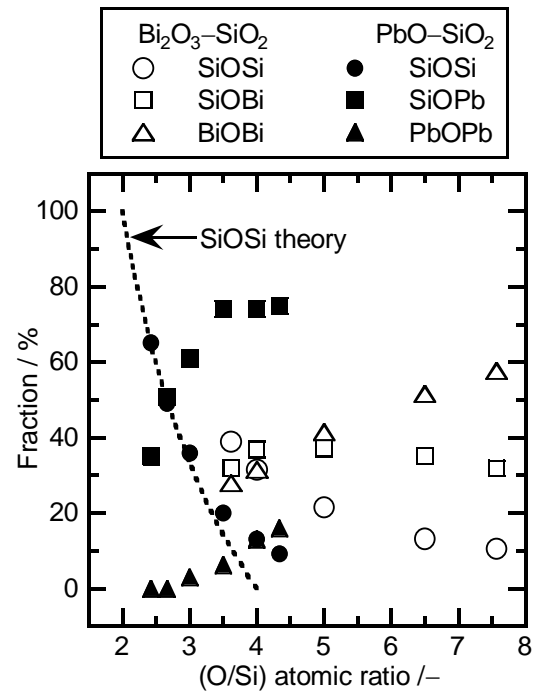


**Fig. 6.** Fraction of various oxygen sites in the glass systems of  $\text{Bi}_2\text{O}_3\text{--SiO}_2$  and  $\text{PbO--SiO}_2$  determined from  $^{29}\text{Si}$  NMR analyses. The dotted line indicates the theoretical amount of typical bridging oxygen in Si–O–Si units, assuming Bi and Pb ions as NWMs.

Among the bismuth silicate crystals,  $Q_0$  units are exclusively present in  $\text{Bi}_4(\text{SiO}_4)_3$  [10] and  $\text{Bi}_{12}\text{SiO}_{20}$  [11], and in  $\text{Bi}_2\text{SiO}_5$  [12], however, only  $Q_2$  units are present, forming continuous  $(\text{SiO}_{2+2})^{2-}$  chains and interlinking  $(\text{Bi}_2\text{O}_2)^{2+}$  double layers (Fig. 7). In the  $\text{Bi}_2\text{SiO}_5$  crystal, there are three crystallographic oxygen sites; O(1) in Si–O–Si (20%), O(2) in

Si–O–Bi (40%) and O(3) in Bi–O–Bi (40%). As shown in Fig. 6, the populations of these oxygen sites in the glasses determined by NMR are almost the same with those in the crystal at  $x = 50$  ( $O/Si = 5.0$ ). As shown in Table 2, the similarity in coordination number around Bi ions is also confirmed at  $x = 50$ . From these results, it is finally concluded that  $50Bi_2O_3 \cdot 50SiO_2$  glass has a similar structure to  $Bi_2SiO_5$  crystal, and it is therefore expected in the  $50Bi_2O_3 \cdot 50SiO_2$  glass that  $BiO_n$  units gather in  $(Bi_2O_2)^{2+}$  double layers sharing their edges and  $Q_2$  units build continuous  $(SiO_3)^{2-}$  chains between the Bi layers.

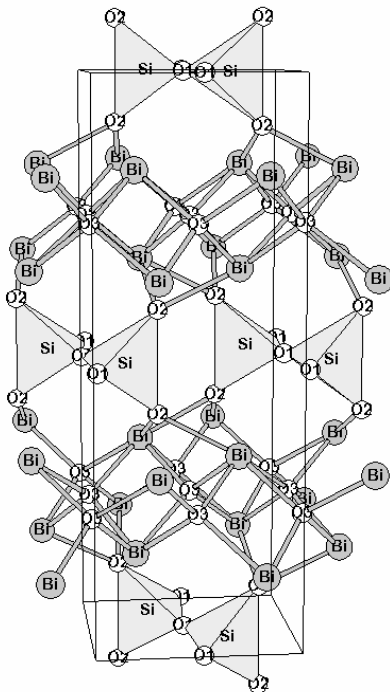


**Fig. 7.** Crystal structure of  $Bi_2SiO_5$ .  
S.G. =  $Cmc2_1(36)$ ,  $a=15.17$ ,  $b=5.47$ ,  $c=5.31$  Å [12].

The  $Q_n$  distributions in  $PbO-SiO_2$  glass obtained in this study show a similar trend to the previous  $^{29}Si$  NMR studies [7–9]. As compared with  $Bi_2O_3-SiO_2$  system (Fig. 6),  $PbO-SiO_2$  system has narrower glass forming region in the scale of ( $O/Si$ ) ratio ( $< 4.5$ ). At ( $O/Si$ )  $\leq 3$ , the Si–O–Si population in  $PbO-SiO_2$  glass is approximately in accordance with the theoretical prediction and Pb–O–Pb bridges are not present, suggesting that Pb ions exclusively act as a network modifier in this region and act as a network former only in the higher ( $O/Si$ ) region. To the best of the authors' knowledge, the quantitative estimation of Pb–O–Pb bridges has never been reported. As for  $Bi_2O_3-SiO_2$  glass, Bi–O–Bi groups are confirmed over the whole glass forming region, indicating that Bi ions prefer to join in the glass

networks. As also shown in Fig. 6, the glass forming region overlaps between  $PbO-SiO_2$  and  $Bi_2O_3-SiO_2$  glasses at ( $O/Si$ ) = 3.5 – 4.5. In this region, the Bi–O–Bi population is much higher than Pb–O–Pb, indicating that Bi ions are much more likely to act as a network former. According to Imaoka et al. [13], Pb ions prefer  $PbO_3$  sites to form  $PbO_3$  chains. The difference in coordination structure between Bi and Pb is a possible reason for the ability for network formation. It should be noted again that the upper limit of ( $O/Si$ ) ratio is different between  $PbO-SiO_2$  and  $Bi_2O_3-SiO_2$  systems but the lower limit of Si–O–Si population is almost the same at 15%. It suggests that Si–O–Si networks are indispensable for the glass formation even when  $BiO_n$  or  $PbO_n$  units join in the glass networks.

## 5. Conclusions

$Bi_2O_3-SiO_2$  system was chosen to investigate the structural role of Bi ions. It was confirmed that Bi ions were present exclusively in a trivalent state. The structural similarities were confirmed between  $50Bi_2O_3 \cdot 50SiO_2$  glass and  $Bi_2SiO_5$  crystal; the similarities in local structure around bismuth and oxide ions were recognized from X-ray radial distribution and  $^{29}Si$  NMR analyses, respectively. In  $50Bi_2O_3 \cdot 50SiO_2$  glass, Bi ions occupied  $BiO_6$  sites, and the  $BiO_6$  units were surrounded by eight  $BiO_6$  units sharing their edges. The oxygen sites were classified into three groups, Si–O–Si, Si–O–Bi and Bi–O–Bi, whose respective populations were estimated as 20%, 40% and 40% in  $50Bi_2O_3 \cdot 50SiO_2$  glass. It was concluded that the Bi–O–Bi bridges formed layers, the Si–O–Si bridges formed chains of  $Q_2$  units, and the bismuthate layers were joined with the silicate chains. The structural characteristics were compared with  $PbO-SiO_2$  system. It was found that the Bi–O–Bi networks existed over the whole glass forming region, while the Pb–O–Pb networks were recognized only in the PbO-rich region at ( $O/Si$ )  $> 3$ . The population of Bi–O–Bi bridges was higher than that of Pb–O–Pb bridges, indicating that Bi ions prefer to act as a network former than Pb ions. In  $Bi_2O_3-SiO_2$  system, however, Bi–O–Bi networks alone could not form glass, and Si–O–Si networks were indispensable for the glass formation.

## Acknowledgments

The authors would like to thank Dr. T. Watanabe of Toyoda Gosei Co., Ltd. for the technical assistance.

## 6. References

- [1] F. Miyaji, T. Yoko, J. Jin, S. Sakka, T. Fukunaga, M. Misawa, *J. Non-Cryst. Solids* **175** (1994) 211.
- [2] T. Watanabe, T. Nanba, Y. Miura, *J. Non-Cryst. Solids* **297** (2002) 73.
- [3] B.V.R. Chowdari, Z. Rong, *Solid State Ionics* **90** (1996) 151.
- [4] L. Baia, R. Stefan, W. Kiefer, J. Popp, S. Simon, *J. Non-Cryst. Solids* **303** (2002) 379.
- [5] A. Shaim, M. Et-tabirou, L. Montagne, G. Palavit, *Mater. Res. Bull.* **37** (2002) 2459.
- [6] S. Matsumoto, T. Nanba, Y. Miura, *J. Ceram. Soc. Japan* **106** (1998) 415 (in Japanese), *J. Ceram. Soc. Jpn. Int. Ed.* **106** (1998) 439 (in English).
- [7] S. Hayakawa, A. Osaka, H. Nishioka, S. Matsumoto, Y. Miura, *J. Non-Cryst. Solids* **272** (2000) 103.
- [8] F. Fayon, C. Bessada, D. Massiot, I. Farnan, J.P. Coutures, *J. Non-Cryst. Solids* **232-234** (1998) 403.
- [9] V.K. Shrikhande, V. Sudarsan, G.P. Kothiyal, S.K. Kulshreshtha, *J. Non-Cryst. Solids* **283** (2001) 18.
- [10] D.J. Segal, P.P. Santoro, R.E. Newnham, *Z. Kristallogr.* **123** (1966) 73.
- [11] S.F. Radaev, V.I. Simonov, Yu.F. Kargin, *Acta Cryst.* **B48** (1992) 604.
- [12] J. Ketterer, V. Krämer, *Neues Jb. Miner. Monat.* **1986**(1) 13.
- [13] M. Imaoka, H. Hasegawa, I. Yasui, *J. Non-Cryst. Solids* **85** (1986) 393.